I.M. BOLESTA,[1] I.N. ROVETSKYJ,[1] M.V. PARTYKA,[2] I.D. KARBOVNYK,[1]
B.YA. KULYK[2]

[1] Ivan Franko National University of Lviv, Faculty of Electronics,
  Chair of Radiophysics and Computer Technologies
  (107, Gen. Tarnavs'kyi Str., Lviv 79017; e-mail: ivan.rovetskyj@mail.ru)
[2] Ivan Franko National University of Lviv, Faculty of Physics,
  Chair of Solid State Physics
  (50, Drahomanov Str., Lviv 79005, Ukraine)

FORMATION OF NANOSTRUCTURES ON THE VdW-SURFACE OF CdI$_2$ CRYSTALS

PACS 61.46.-w, 68.47.Fg

Morphological characteristics of nano-sized defects and nanostructures formed on the surface of CdI$_2$ layered crystals have been studied, and the processes of their growth under conditions close to the thermodynamic equilibrium have been analyzed. The formation of nano-sized structures – nanoclusters and nanopores – emerging on the CdI$_2$ surface after holding the crystals in air for some time is revealed for the first time. A mechanism of cluster formation is proposed, which includes a number of stages of cluster growth; these are the nucleation, formation of separate noninteracting nanoaggregates, and association of the latter into agglomerates. The major morphometric characteristics of nanostructures – their average radius and height, and the average distance between the nearest neighbors – are analyzed.

K e y w o r d s: nanoclusters, nanopores, Van der Waals surfaces, Bridgman–Stockbarger method.

1. Introduction

High energy-gap CdI$_2$ crystals belong to halogenides of the MX$_2$ type with a layered structure. The latter is formed by a dense hexagonal packing of iodine atoms. Half a number of octahedral cavities in the structure are occupied by cadmium atoms arranged in layers. Interaction between cadmium atoms, which possess a strong polarization ability, and iodine ones, which are easily polarized, results in the formation of ternary layers I–Cd–I with strong ionic-covalent bonds. The energy of the latter evaluated by the dissociation energy of a molecular Cd–I bond amounts to 50 kcal/mol [1]. The neighbor ternary layers are coupled with each other by weak Van der Waals bonds with an energy of 0.4 kcal/mol, so that the anisotropy of bond forces Cd–I/I–I amounts to about 125 [1]. This circumstance is responsible for the extremely high anisotropy of mechanical properties of CdI$_2$ crystals, which manifests itself in a perfect cleavage of the crystal along the (0001) basal planes [2]. As a result, iodine atoms form ideal surfaces, which are called Van

der Waals (VdW) ones and which can be obtained by cleaving the crystal along its basal planes.

A low density of dangling bonds at VdW surfaces of layered crystals predetermines their application as substrates for growing molecular, organic, and metallic nanostructures [3–5], obtaining semiconductor heterostructures by the method of VdW heteroepitaxy [6, 7], as well as a nanorelief standard in the metrology of nanoobjects [8].

The processes of nanostructure formation on VdW surfaces are intensively studied for layered narrow-gap crystals of group A^{III}B^{V} such as GaSe [9, 10] and InSe [11, 12], as well as In$_x$Se$_{1-x}$ alloys [13–16]. As far as we know, similar researches for high energy-gap layered crystals belonging to the MX$_2$ group are absent.

There are some works devoted to the microscopic research of the surface of layered CdI$_2$ crystals grown, as a rule, from aqueous solutions. Using the methods of optical, tunnel (TEM), and scanning (SEM) electron microscopy, new elements were detected in the growth spirals that are formed on the basal (0001) faces of CdI$_2$ crystals. Namely, there emerge substeps with heights equal to or multiple of the c-period of the structure. The horizontal interstep distance

was found to be multiple of the lattice parameter a [17–19]. A mismatch between the height of a growth spiral and the lattice period c was also revealed. It was explained in [20] as a result of the interaction between noncompensated bonds at the I–Cd–I layer edges (steps) and the crystal surface, which stimulated a reduction of the I–Cd–I sandwich width from 0.343 to 0.310 nm.
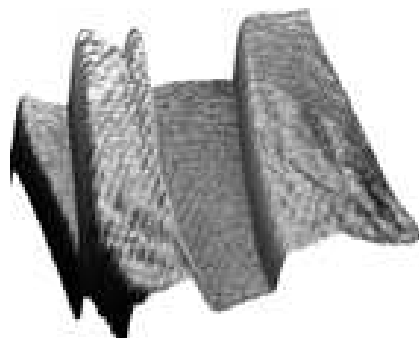
While studying the surface morphology of CdI$_2$ crystals grown from the aqueous solution using the atomic-force microscopy (AFM) method, linear steps (terraces), dips, and islands were revealed. The CdI$_2$ surface is atomically planar between those elements; in particular, the relief inhomogeneities were found to equal 10.2 and 4.7 Å [21]. A long-term annealing (for about 44 h) in air gave rise to the appearance of craters (dips) and pyramid-shape elements with a height of 20–50 nm on the crystal surface [22].

In work [23], the formation of nanoparticles in CdI$_2$ under the action of an electron beam was found. The cited authors assumed that the particles emerged owing to the recrystallization of the specimen material evaporated under the action of the electron beam. Those particles are mainly metallic, because the ratio Cd:I in them amounts to 2:1, in contrast to 1:1.5 in stoichiometric compounds. Metallic clusters were also found in non-stoichiometric CdI$_2$ crystals that were grown from the melt [24].

From the presented data, it follows that the processes of formation of nano-sized defects and nanostructures on the VdW surface of layered CdI$_2$ crystals have practically been not analyzed. Therefore, in this work, the AFM method is applied to study nano-sized defects and nanostructures that are formed on the surface of crystals, and the processes of their growth under conditions close to thermodynamically equilibrium ones are analyzed.

2. Experimental Specimens and Technique

Cadmium iodide (CdI$_2$) single crystals were grown from the melt using the Bridgman–Stockbarger method. The raw substance was preliminarily purified with the use of the zone melting technique. Simultaneously with the growing of a single-crystal specimen, thin single-crystalline CdI$_2$ plates were formed from the gas phase on the walls in the upper part of the ampoule. The surfaces of those plates were not subjected to a preliminary mechical treatment.

Fig. 1. Image of the morphology of the as-cleaved surface of CdI$_2$ crystal after a detachment of the plane with the use of an adhesive tape. The image size is 20×20 μm^2, the z-range is 24.40 nm

"Old" and as-cleaved VdW surfaces of CdI$_2$ crystals, either grown from the melt or obtained from the gas phase, are studied. The "old" surfaces were formed when the specimens were kept in air in dark for a long time (about a month and longer). Fresh cleavages of the crystals were obtained by removing the upper layers with the use of a razor blade or an adhesive tape.
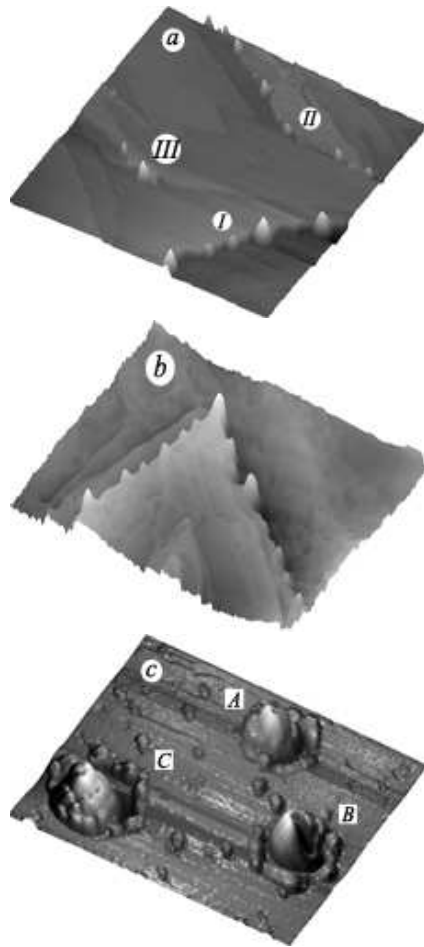
The morphology of the VdW surface of single crystals was researched using the methods of contact and semicontact atomic-force microscopy with the help of a Solver P47-PRO microscope. The design of this model of scanning probe microscope allowed only one type of scanning to be realized, which is called the "scanning-by-sample" mode. The probe tip radius did not exceed 10 nm. The vertical resolution of the device was 1 Å.

The dimensions of specimens were not smaller than 5×5 mm^2, and their thickness was 0.5 to 1 mm. The specimens were mounted on special polycrystalline substrates with the use of a double sided adhesive tape.
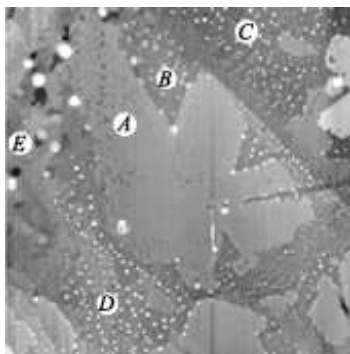
For processing the digital electron-microscopy images, we created a software program in the Mathlab language, which enabled us to obtain the numerical characteristics of researched nanostructures.

3. Research Results and Their Discussion

A typical image of the morphology of an as-cleaved (with the use of an adhesive tape) VdW surface of CdI$_2$ crystal grown from the melt is exhibited in Fig. 1. One can see that there are atomically smooth sections–terraces separated by steps–on the crystal

Fig. 2. Formation of nanostructures at dislocations (*a* and b) and in nanopores (*c*). The image size is 10×10 (*a*), 8×10 (*b*), and 2.6×3.1 μm^2 (*c*). The *z*-range is 45.80 (*a*), 37.20 (*b*), and 46.6 nm (*c*)

Fig. 3. Formation of cluster nanosystems on the "old" surface of CdI$_2$ crystal grown from the melt. The image size is 10×10 μm^2, the *z*-range is 30.23 nm

surface. The formation of terraces on the surface can be explained by the fact that the stratification of CdI$_2$ crystal occurs along VdW planes with a minimum imperfection, where the binding forces between the surfaces are the weakest (by magnitude, they are close to VdW forces), which is inherent to layered crystals [8]. Therefore, the steps can be considered as certain defect boundaries formed at the crystal growing (e.g., edge dislocations). The step heights in Fig. 1 vary within the limits 7–11 nm. Since the parameter c for CdI$_2$ equals 0.687 nm [20], it follows that the steps are composed of approximately 10–15 ternary sandwiches I–Cd–I.
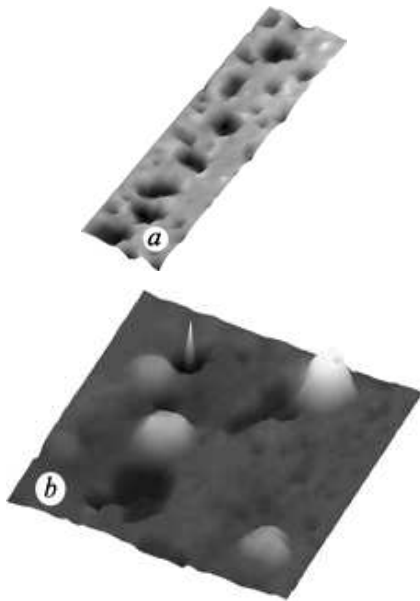
In Fig. 2, *a*, the morphology of an as-cleaved surface after holding the crystal in air for about 1 h is shown. On this surface, one can observe steps (*I*, *II*, and III in Fig. 2, *a*) with a complicated configuration. They intersect one another at the angles equal to or multiple of 60°, which corresponds to the dense hexagonal atomic packing in the CdI$_2$ layered crystal. For example, the angle between steps in Fig. 2, *b* is equal to approximately 64°, whereas the angle between steps *II* in Fig. 2, *a* to approximately 125°.

Holding the as-cleaved VdW surface in air resulted in the formation of pyramid-shape nanostructures on it. We found that such nanostructures are formed only along the steps. The average radius of emerging clusters was $r_c = 120.9$ nm, and their average height equaled $h_c = 18.1$ nm, which was larger than the heights of steps *I*, *II*, and III in Fig. 2,*a* (9–12, 3–6, and 3–4 nm, respectively).

On the CdI$_2$ surface cleaved with the help of a razor blade 3 days before the measurement, we managed to register the appearance of hexagonal nanopores, in which nanoclusters were formed (Fig. 2, *c*). The hexagonal shape of nanopores also corresponded to the hexagonal CdI$_2$ structure. The geometrical sizes of three nanostructures labeled in Fig. 2, *c* as *A*, *B*, and *C* are quoted in Table 1.

Table 1. **Dimensions of nanostructures formed on the as-cleaved CdI$_2$ surface (Fig. 2, *c*)**

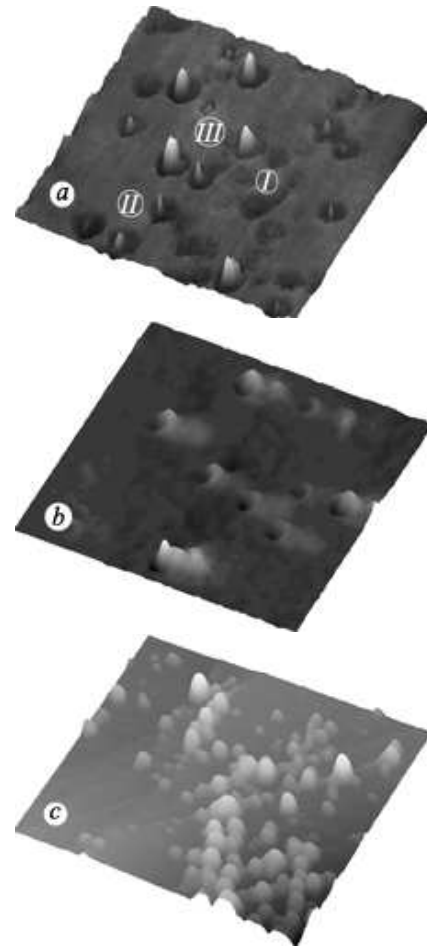| Pore (cluster)	Pore diameter, nm	Cluster diameter, nm	Cluster height, nm
A	453.1	627.2	41.1
B	644.3	655.2	37.4
C	849.2	776.1	32.7

Fig. 4. *a*) Nanopore and (*b*) nanocluster formations on the "old" CdI$_2$ surface. The image size is 3.5×0.75 (*a*) and 2×2 μm^2 (*b*). The *z*-range is 4.95 (*a*) and 30.23 nm (*b*)

Figure 3 demonstrates the AFM image for the morphology of a certain section on the "old" surface of CdI$_2$ crystal grown from the melt. As was in the case of as-cleaved surfaces, the "old" crystal surface contains atomically smooth sections–terraces–where clusters have not been formed yet (section *A* in Fig. 3). We also detected sections, on which the formation of a significant number of clusters–cluster nanosystems–took place (sections *B* to *E* in Fig. 3).

In Table 2, numerical values for the parameters of clusters formed in areas of 2×2 μm^2 each in sections *B* to *E* (see Fig. 3) are presented. The clusters formed in section *B* had the smallest average height $h_c = 3.1$ nm. In sections *C* and *D*,

Table 2. **Morphometric parameters of clusters formed on sections *B*, *C*, *D*, and *E* in Fig. 3**
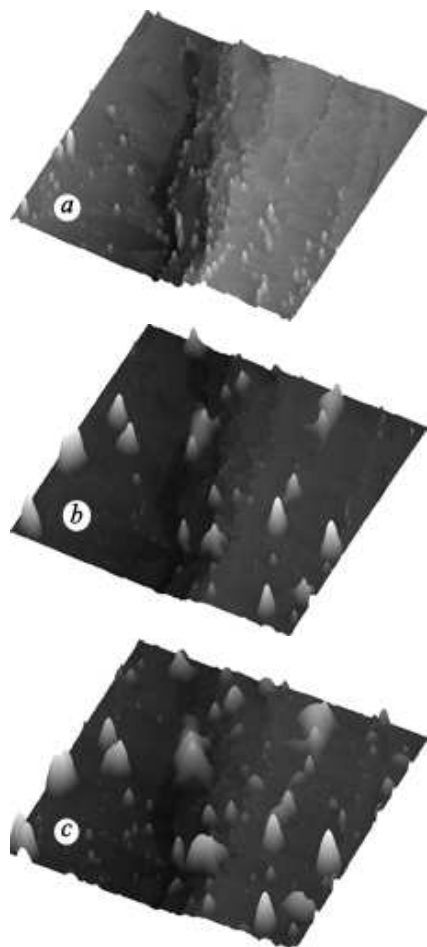
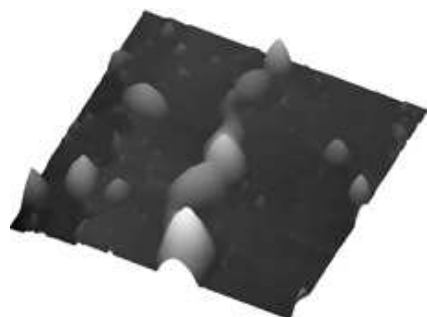| Section	Number of clusters	Average cluster height, nm	Average cluster radius, nm	DNN, nm
B	27	3.1	51.1	266.1
C	54	5.2	34.1	174.1
D	54	6.9	39.1	194.1
E	4	13.3	139.9	831.2

Fig. 5. (*a*) Dynamics of the cluster formation, (*b*) cluster formation at the pore edges, and (*c*) interaction between clusters. The image size is 2×2 (*a*), 1×1 (*b*), and 5×5 μm^2 (*c*). The *z*-range is 3.15 (*a*), 2.43 (*b*), and 35.80 nm (*c*)

their number was the largest, $n = 54$, and they were arranged here more densely, which was testified by a reduction of the average distance to the nearest neighbor (DNN), $d_c = 174.1$ nm. The smallest number of clusters, $n = 4$, was observed in section *E*. However, here they had the biggest geometrical sizes, $h = 13.3$ nm and $r_c = 139.9$ nm, and were located most distantly from one another, $d_c = 831.2$ nm. The results obtained for the morphometric parameters of clusters can be explained if we assume that, in those sections, they are at different stages of stochastic growth.
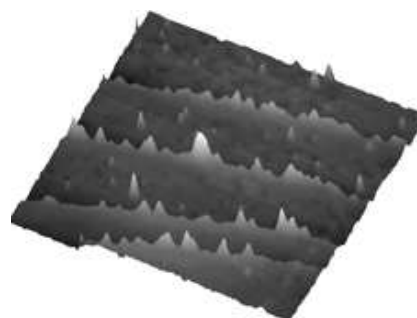
On the "old" surface terraces, we detected the emergence of "negative" clusters – nanopores (Fig. 4, *a*) –

Fig. 6. Evolution of the nanostructure formation on the CdI$_2$ surface after its holding in air for 3 h (*a*), 3 days (*b*), and 6 days. The image size is 5×5 μm^2. The z-range is 23.0 (*a*), 55.7 (*b*), and 61.1 nm (*c*)

Fig. 7. Formation of cluster agglomerates on the CdI$_2$ surface after the 6-day holding in air. The image size is 2×2 μm^2. The z-range is 48.0 nm

Fig. 8. Formation of cluster agglomerates on the "old" surface of CdI$_2$ crystal obtained from the gas phase. The image size is 6×6 μm^2. The z-range is 5.31 nm

with other nanoobjects developing inside them and at their boundaries (Fig. 4, *b*). The depths of nanopores in Fig. 4, *a* vary within the interval of 2–4 nm. The height of a nanoobject in the pore depicted in Fig. 4, *b* equals 29.8 nm, and the pore depth is 7.7 nm. The average height of four nanoobjects emerging at the nanopore boundaries (Fig. 4, *b*) is about 14 nm, and their average depth is about 4 nm.

In Fig. 5, *a*, we marked three sections – *I, II*, and *III* – which reflect the dynamics of cluster formation on the "old" VdW surface of CdI$_2$ crystals grown from the gas phase. Only nanopores are observed in section *I*. In section *II*, clusters emerge in the pores and fill them in the course of their formation (section *III*). The average heights of nanoobjects formed in those surface sections are equal to about 1.3 and 2.6 nm, respectively. The diameter and the depth of nanopores amount to 200 and 0.5 nm, respectively, at every stage of cluster growth.

Similarly to the case of the surface formation from a melt, the nucleation and the formation of clusters on the surface from the gas phase are observed not

Table 3. **Morphometric parameters of clusters after holding the crystal in air for 3, 70 (3 days), and 140 h (6 days)**

Cluster parameters	3-h holding period	3-day holding period	6-day holding period
Number	148	55	61
Average height, nm	4.9	17.3	17.3
Average radius, nm	26.7	77.6	86.7
DNN, nm	183.4	406.5	385.2

only inside the pores, but also at their boundaries (Fig. 5, *b*). However, the dimensions of clusters and nanopores on the surface of such crystals are considerably smaller. An example is illustrated in Fig. 5, *b*, where clusters 0.7 nm in height are formed at the boundaries of pores 0.3 nm in depth. In the section shown in Fig. 5, *c*, clusters already filled the pores completely and start to interact with one another. Their average height amounts to $h_c = 6.6$ nm at this stage.

The experimental data evidence that, after the clusters have been nucleated, they grow (Figs. 3 and 5, *a*) and interact (Fig. 5, *c*), when the crystal is held in air. To confirm those experimental facts, we studied, within a week period, the evolution dynamics of cluster formation on the same section of the as-cleaved (with the use of a razor blade) VdW surface of a CdI₂ crystal grown from the melt. The first measurement was carried out after the crystal had been held in air for about 3 h (Fig. 6, *a*). This time interval turned out sufficient for nanoobjects to be formed along the linear steps. In approximately 70 h (3 days) after cleaving the surface, a substantial growth of clusters and their interaction– namely, their coagulation–were registered (Fig. 6, *b*). At the final stage of this process, the number of clusters diminishes, but they become bigger (Table 3). The third measurement of the morphology of the selected surface section was carried out in approximately 140 h (6 days) after the surface cleavage (Fig. 6, *c*). It showed an increase in the number of nanoobjects due to the formation of new (smaller) clusters (Table 3).

We detected another type of interaction between the clusters, their "sintering", which results in the formation of agglomerates, i.e. structures with much larger dimensions (Fig. 7). The formation of agglomerates along the linear steps was also observed on the surface of a crystal grown from the gas phase (Fig. 8). The average height of clusters that the agglomerates consisted of (Fig. 8) was equal to $h_c = 1.9$ nm.

A strong dependence of the number of nanoobjects on the time of specimen holding in air testifies, first of all, to an important role of water vapor and, possibly, oxygen in the process of their formation. Adsorption of H₂O molecules onto defect sites of the VdW surface (e.g., edge and/or screw dislocations) should be regarded as the initial stage of this process, which invokes the stage of crystal dissolution. As a result, the

surface defects hexagonal in shape emerge, which is typical of the CdI₂ hexagonal structure. In a vicinity of those defects, the bonds between metal atoms become broken. As a result, free Cd atoms appear, which interact with atmospheric oxygen and become a "building material" for nanoobjects.

The obtained experimental results allow the mechanism of cluster formation on the CdI₂ surface to be proposed. It consists in that defects-nanopores are formed at the initial stage; individual nanoclusters, which do not interact with one another, emerge inside them and at their boundaries; in the course of their formation, the clusters completely fill the pores. This stage of nanoobject growth can be observed the most pronounced on the "free" VdW surface of CdI₂ crystals obtained from the gas phase. At the next stage, the clusters start to interact with one another. Owing to the coagulation process, their number diminishes, and the clusters become much bigger. At the last stage of the process, the nucleation of new, smaller, clusters increases their number, and the process of their "sintering" is observed. As a result, the intercluster boundaries disappear, and the clusters join to form agglomerates.

4. Conclusions

To summarize, our researches of the morphology of "old" and as-cleaved surfaces of CdI₂ crystals grown from both the melt and the gas phase, which were carried out with the use of atomic-force microscopy methods, have revealed the formation of nano-sized structures–nanoclusters and nanopores–on the VdW surfaces. The morphometric parameters of those structures, such as the height and the radius, are determined. It is established that the linear steps and the nanopores are the centers of nanocluster nucleation. According to the results of our researches obtained for the time evolution of cluster formation on the VdW surfaces of CdI₂ crystals, a mechanism of cluster growth and interaction of clusters with one another is proposed.

1. M.A. Wahab and G.C. Trigunayat, Solid State Commun. **36**, 885 (1981).
2. Q.-J. Liu, Z.-T. Liu, and L.-P. Feng, Phys. Status Solidi B **248**, 1629 (2011).
3. K. Ueno, K. Sasaki, K. Saiki, and A. Koma, Jpn. J. Appl. Phys. **38**, 511 (1999).

4. S.I. Drapak, A.P. Bakhtinov, S.V. Gavrilyuk, Yu.I. Prilut-skii, and Z.D. Kovalyuk, Fiz. Tverd. Tela **48**, 1515 (2006).

5. W. Jaegermann, C. Pettenkofer, and B.A. Parkinson, Phys. Rev. B **42**, 7487 (1990).

6. E. Wisotzki, A. Klein, W. Jaegermann, Thin Solid Films **380**, 263 (2000).

7. O. Lang, R. Schlaf, Y. Tomm, C. Pettenkofer, and W. Jaegermann, J. Appl. Phys. **75**, 7805 (1994).

8. A.I. Dmitriev, Zh. Tekhn. Fiz. **82**, 114 (2012).

9. A.P. Bakhtinov, V.N. Vodop'yanov, E.I. Slyn'ko, Z.D. Kovalyuk, and O.S. Litvin, Pis'ma Zh. Tekhn. Fiz. **33**, No. 2, 80 (2007).

10. A.P. Bakhtinov, Z.R. Kudrinskii, and O.S. Litvin, Fiz. Tverd. Tela **53**, 2045 (2011).

11. A.P. Bakhtinov, Z.D. Kovalyuk, O.N. Sidor, V.N. Katerinchuk, and O.S. Litvin, Fiz. Tverd. Tela **49**, 1497 (2007).

12. A.I. Dmitriev, V.V. Vishnyak, G.V. Lashkarev, V.L. Karbovskii, Z.D. Kovalyuk, and A.P. Bakhtinov, Fiz. Tverd. Tela **53**, 579 (2011).

13. O.A. Balitskii, V.P. Savchyn, and Ya.M. Fiyala, Funct. Mater. **12**, 206 (2005).

14. O.A. Balitskii, Mater. Lett. **60**, 594 (2006).

15. O.A. Balitskii, J. Electr. Microsc. **55**, 261 (2006).

16. O.A. Balitskii, V.P. Savchyn, B. Jaeckel, and W. Jaegerman, Physica E **22**, 921 (2004).

17. R. Singh, S.B. Samanta, A.V. Narlikar, and G.C. Trigunayat, J. Cryst. Growth **204**, 233 (1999).

18. R. Singh, S.B. Samanta, A.V. Narlikar, and G.C. Trigunayat, Bull. Mater. Sci. **23**, 131 (2000).

19. B. Kumar and N. Sinha, Cryst. Res. Technol. **40**, 887 (2005).

20. R. Singh, S.B. Samanta, A.V. Narlikar, and G.C. Trigunayat, Surf. Sci. **422**, 188 (1999).

21. N.-Y. Cui, N.M.D. Brown, and A. McKinley, Appl. Surf. Sci. **152**, 266 (1999).

22. R. Popovitz-Biro, N. Sallacan, and R. Tenne, J. Mater. Chem. **13**, 1631 (2003).

23. N. Sallacan, R. Popovitz-Biro, and R. Tenne, Solid State Sci. **5**, 905 (2003).

24. I.M. Bolesta, R.I. Gryts'kiv, Yu.P. Datsyuk, and B.M. Pavlyshenko, Ukr. Fiz. Zh. **48**, 1 (2003).

І.М. Болеста, І.М. Ровецький,
М.В. Партика, І.Д. Карбовник

ПРОЦЕС ФОРМУВАННЯ НАНОСТРУКТУР
НА ВдВ-ПОВЕРХНІ КРИСТАЛІВ CdI$_2$

Р е з ю м е

Досліджено морфологічні характеристик нанорозмірних дефектів і наноструктур, сформованих на поверхні шаруватого кристала CdI$_2$, а також проаналізовано процеси їх росту в умовах, близьких до термодинамічно рівноважних. У результаті проведених досліджень вперше виявлено формування на поверхні CdI$_2$ нанорозмірних структур – нанокластерів та нанопор, що утворюються внаслідок витримування кристала на повітрі протягом деякого часу. Запропоновано механізм формування кластерів, який охоплює декілька стадій їхнього росту: зародження, формування окремих наноутворень, що не взаємодіють між собою та їх об'єднання у агломерації. Проаналізовано основні морфометричні характеристики наноструктур: середній радіус та висоту, середню відстань до найближчого сусіда.